Rational Truncation of Aptamer for Ultrasensitive Aptasensing of Chloramphenicol: Studies Using Bio-Layer Interferometry

Richa Sharma , Monali Mukherjee , Praveena Bhatt , KSMS Raghavarao *

Posted Date: 29 April 2023

doi: 10.20944/preprints202304.1208.v1

Keywords: Antibiotics; affinity; biosensing; food; interferometry; nanoparticles

Article

Rational Truncation of Aptamer for Ultrasensitive Aptasensing of Chloramphenicol: Studies Using Bio-Layer Interferometry

Richa Sharma [1,2], Monali Mukherjee [2,3], Praveena Bhatt [2,3] and KSMS Raghavarao [1,2,4,*]

[1] Department of Food Engineering, CSIR- Central Food Technological Research Institute (CFTRI), Mysore-570020, India
[2] Academy of Scientific and Innovative Research (AcSIR), CSIR-CFTRI, India
[3] Department of Microbiology and Fermentation Technology, CSIR-CFTRI, India
[4] Department of Chemical Engineering, IIT-Tirupati, Tirupati – 517506, India
* Correspondence: raghava@iittp.ac.in, ksmsraghavarao60@gmail.com; Tel.: Phone: + 91- 821-2513910; Fax: + 91-821-2517233

Abstract: Aptamers are excellent choices for selective detection of small molecules. However, the previously reported aptamer for chloramphenicol suffers from low affinity, probably as a result of steric hindrance due to its bulky nature (80 nucleotides) leading to lower sensitivity in analytical assays. The present work was aimed at improving this binding affinity by truncating the aptamer without compromising its stability and three-dimensional folding. Shorter aptamer sequences were designed by systematically removing bases from each or both ends of the original aptamer. Thermodynamic factors were evaluated computationally to give insights into the stability and folding patterns of the modified aptamers. Binding affinities were evaluated by bio-layer interferometry. Among the 11 sequences generated, one aptamer was selected based on its low dissociation constant, length and regression of model fitting with association and dissociation curves. The dissociation constant could be lowered by 86.93% by truncating 30 bases from the 3′ end of the previously reported aptamer. The selected aptamer was used for gold nanospheres based colorimetric detection of chloramphenicol in real samples. The detection limit could be reduced 32.87 times (1.673 pg mL^{-1}) using the modified length aptamer, indicating its improved affinity as well as suitability in real sample analysis for ultrasensitive detection of chloramphenicol.

Keywords: antibiotics; affinity; biosensing; interferometry; nanoparticles

1. Introduction

Chloramphenicol (CAP, Protein Database ID: 1NJI, IUPAC: 2,2-dichloro-n-[1,3-dihydroxy-1-(4-nitrophenyl)propan-2-yl]acetamide) is a bacteriostatic antimicrobial which finds wide application in treatment of acutely infected animals. However, intake of the antibiotic by humans has potential ramifications on health, leading to blood dyscrasias, bone marrow suppression, blue-baby syndrome and resistance [1]. Thus, the extra-label use of CAP in food-producing animals (such as, cattle, poultry, fish and honeybees) is strictly forbidden under the Animal Medicinal Drug Use Clarification Act [2]. Despite such regulations CAP has been found in domestic and exported food products, in enzymes added to fodder as well as in the environment (animal excreta) creating considerable health and economic losses [3]. Conventional methods for monitoring of CAP rely on solvent-based and lengthy procedures such as HPLC (limit of detection = 21.4 ng mL^{-1}) [4]. Since regulations have zero-tolerance policy for CAP, detection methods should be able to identify even minute traces.

Aptamers have been proven to be competent bio-recognition and targeting molecules [5]. They provide specificity, tunable synthesis and modifiability. Several aptasensing platforms have been developed for CAP [6–18]. However, many of them involve multiple steps, several sets of biomolecules and nanoparticles, and modest sensitivity. Hence, we attempted to optimize a simple

Preprints (www.preprints.org) | NOT PEER-REVIEWED | Posted: 29 April 2023 doi:10.20944/preprints202304.1208.v1

visual assay for screening of CAP [19] where it competes with nanosphere surfaces to bind to the aptamer. The quantification curve showed poor resolution and detection limit in real samples. We hypothesize that this is due to the bulky structure of the aptamer which prevents efficient target binding, adequate conformational change and therefore insufficient nanoparticle aggregation.

The present study was therefore aimed at improvement of the sensitivity of colorimetric aptasensing of CAP, by increasing binding affinity of the aptamer. This is difficult to achieve by *de novo* aptamer selection [20] although some success was achieved by Duan et al. 2016 [21]. We attempted rational truncation of reported aptamer. The designed truncated aptamers were computationally examined for stability, thermodynamic feasibility and subjected to binding affinity studies using biolayer interferometry (BLI). The oligonucleotide with lowest dissociation constant (K_d) exhibited considerable reduction in detection limit in real samples compared to the original aptamer. This is a first attempt to truncate the CAP aptamer to improve bio-affinity and biosensing. This contributes significantly to the development of simple "yes/no" test for CAP in food samples. In addition, use of biolayer interferometry for studying nucleic acid-small molecule specificity studies is being reported for the first time.

2. Materials and Methods

2.1. Materials

Tetrachloroauric acid trihydrate, trisodium citrate, chloramphenicol (CAP), original and curtailed aptamers (biotin labelled) were procured from Sigma Aldrich (USA). Dehydrated aptamers were subjected to a brief spin, suspended in water and stored at -20° C. The surface-modified probes used for the BLI assay were provided by the manufacturer of the BLI instrument Octet RED96 (ForteBio, Pall Life Sciences Corp., USA). The Super Streptavidin (SSA) modification is especially suited for small molecular studies. Transmission Electron Micrograph images were obtained using Titan Themis 300kV, FEI (Thermo Scientific Labs Pvt Ltd.) housed at Micro Nano Characterization Facility, Indian Institute of Science, Bangalore. Binding buffer for CAP (100 mM NaCl, 20 mM Tris–HCl, 2 mM $MgCl_2$, 5 mM KCl, 1 mM $CaCl_2$, 0.02 Tween 20, pH 7.6) was used for determining the curves for baseline, association and neutralization in the BLI protocol, whereas 2 M $MgCl_2$ was used for dissociation. All salts used were extra pure and purchased from Ranbaxy Fine Chemicals Limited, India. MilliQ Millipore plus water was used as solvent. Softwares tools used were Mfold (http://unafold.rna.albany.edu/) and Data Acquisition Octet (ForteBio, Pall Life Sciences Corp., USA).

2.2. Methods

2.2.1. Truncation of the original aptamer

The truncation design followed removal of nucleotide stretches (5, 20, 30 and 40 bases) from one or both ends of the original aptamer (80 bases) [22] without interfering with the consensus binding region (Table 1).

Table 1. Aptamer sequences with curtailed lengths[a].

Sl. no	Sequence (5′ → 3′)	No. of bases removed	Terminal/ Seq base numbers
1	***AGCAGCACAGAGGTCAGATG***ACTTCAGTGAGTTGTCCCACG GTCG**GCGAG**TCGGTGGTAG***CCTATGCGTGCTACCGTGAA*** **(original)**	0	- 1 to 80
2	***CACAGAGGTCAGATG***ACTTCAGTGAGTTGTCCCACGGTCG**G CGAG**TCGGTGGTAG***CCTATGCGTGCTACCGTGAA***	5	5′ 6 to 80
3	***AGCAGCACAGAGGTCAGATG***ACTTCAGTGAGTTGTCCCACG GTCG**GCGAG**TCGGTGGTAG***CCTATGCGTGCTACC***	5	3′ 1 to 75

Preprints (www.preprints.org) | NOT PEER-REVIEWED | Posted: 29 April 2023 doi:10.20944/preprints202304.1208.v1

4	***CACAGAGGTCAGATG***ACTTCAGTGAGTTGTCCCACGGTCG**G CGAG**TCGGTGGTAG***CCTATGCGTGCTACC***	10	5′& 3′ 6 to 75
5	ACTTCAGTGAGTTGTCCCACGGTCG**GCGAG**TCGGTGGTAG***C CTATGCGTGCTACCGTGAA***	20	5′ 21 to 80
6	***AGCAGCACAGAGGTCAGATG***ACTTCAGTGAGTTGTCCCACG GTCG**GCGAG**TCGGTGGTAG	20	3′ 1 to 60
7	ACTTCAGTGAGTTGTCCCACGGTCG**GCGAG**TCGGTGGTAG	40	5′ & 3′ 21 to 60
8	GTTGTCCCACGGTCG**GCGAG**TCGGTGGTAG***CCTATGCGTGCT ACCGTGAA***	30	5′ 31 to 80
9	***AGCAGCACAGAGGTCAGATG***ACTTCAGTGAGTTGTCCCACG GTCG**GCGAG**	30	3′ 1 to 50
10	GTTGTCCCACGGTCG**GCGAG**	60	5′ & 3′ 31 to 50
11	GGTCG**GCGAG**TCGGTGGTAG***CCTATGCGTGCTACCGTGAA***	40	5′ 41 to 80

[a] Bold underlined bases signify the 5′-base consensus sequence that binds to CAP. Bold and italic bases at 5′ and 3′ ends are primer binding sites for SELEX protocol. The rest are random sequences for the SELEX library.

2.2.2. Secondary structures of curtailed oligonucleotides

The most popular tool for predicting folding of single stranded oligonucleotides in solution is Mfold [23]. For the present work, sequences, experimental buffer details and temperature were used as constraints to obtain secondary structures and circular plots of nucleotide hybridization.

2.2.3. Energetics and stability of curtailed oligonucleotides

For determining energetics, the curtailed nucleotide sequences and binding conditions ($[Na^+]$ = 0.1 M and $[Mg^{2+}]$ = 0.002 M) were entered as queries in Mfold software. The selected output parameters were melting temperature (Tm), total Gibbs free energy change of folding (ΔG) at 37°C, enthalpy change (ΔH) and entropy change (ΔS). The program was tuned to give standard errors of approximately ±5%, ±11% and ±4°C for ΔG, ΔS and Tm, respectively [24,25].

2.2.4. Biolayer interferometry studies on binding affinity

The biotinylated oligonucleotides were suspended in appropriate buffer and added to a 96-well black microplate (Figure S1). They were then subjected to interferometric analysis. The BLI analysis follows a series of steps involving loading of aptamer onto probes, its attachment to analyte and subsequent dissociation (refer Supplementary Information).

2.2.5. Aptasensing of CAP

The aptamer with the highest binding affinity in BLI studies was selected for nanosphere aggregation assay of CAP. Original aptamer was used for comparison. Gold nanospheres were synthesized in lab by citrate reduction of tetraaurochloric acid and then protected from salt-induced aggregation by aptamers (red suspension). In presence of CAP, aptamers selectively bound to their target, releasing nanospheres to be aggregated (blue suspension). The measurable colorimetric change was used for quantification of CAP. The detection was performed with optimized concentrations of assay buffer (16.67% v/v), gold nanospheres (66.67% v/v of as-prepared colloid), NaCl (44 mM) aptamers (0.044 μM), and incubation time (25 minutes) [22].

2.2.5.1. Performance of the assay

The ratios of plasmon absorbances of gold nanospheres at 610 nm and 520 nm (triplicate readings) for different concentrations of CAP were plotted and linear range was determined. The

 doi:10.20944/preprints202304.1208.v1

limit of detection (LOD) and limit of quantification (LOQ) were ascertained using following equations:

$$LOD = 3S_b/m$$

$$LOQ = 10S_b/m,$$

where S_b is standard deviation of the signal for blank and m is slope of linear regression curve.

2.2.5.2. Validation in real samples

Five grams honey were diluted with 15 mL water and divided into fifteen aliquots. Three aliquots for each of the five samples were analysed - one without artificial contamination and four artificially contaminated samples with 10, 50, 100, 1000 pg mL^{-1} CAP. The mixture was vortexed until homogeneity and filtered (0.45 μm) to remove denatured proteins. The responses of the colorimetric biosensing were validated by HPLC analysis.

2.2.5.3. Reproducibility and specificity

All experiments were conducted in triplicates on the same day. Intra-day and inter-day precision were established by analysing a single concentration of CAP 10 times on a single day and once every 10 consecutive days within the same laboratory. A number of analogues of CAP (florfenicol, thiamphenicol, CAP succinate at 100 ng/mL concentration)) were subjected to the aptasensing method, to determine its specificity.

3. Results and Discussion

3.1. Truncation of the original aptamer

Aptamers of sequence length between 40-50 bases have been successfully used for biosensing of low molecular weight targets such as theophylline, cocaine and ochratoxin A. [26,27]. Overly long aptamers tend to bind non-specifically. CAP is a small molecule with molar mass 323 g/mol, whereas its reported aptamer is 80 bases long (Figure 1). Therefore, we attempted to curtail the aptamer expecting to increase its binding affinity, as has been done for other analytes [28,29].

The primer-binding terminal bases of original aptamer (Sequence 1) does not participate in secondary structures, whereas the consensus (46 – 50 bases) was essential. Therefore, rational truncation design was started with 5 bases (Sequences 2, 3 and 4), followed by 20 bases (Sequences 5, 6 and 7), 30 bases (Sequences 8, 9 and 10) from either and both terminals and finally 40 bases only from 5′ end (Sequence 11).

Preprints (www.preprints.org) | NOT PEER-REVIEWED | Posted: 29 April 2023 doi:10.20944/preprints202304.1208.v1

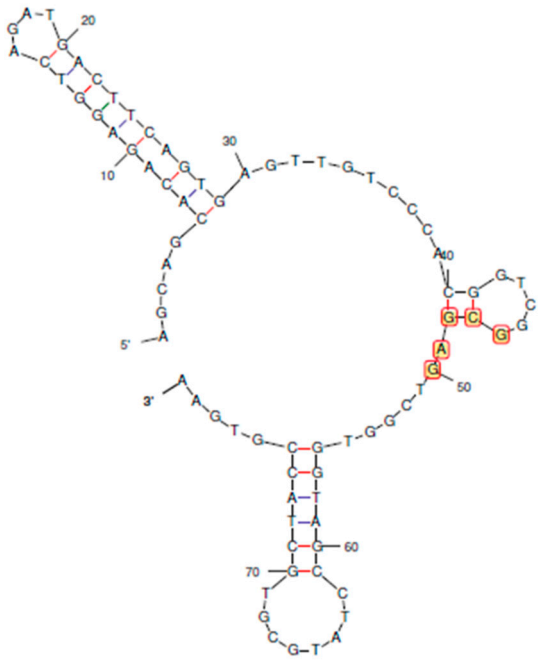

Figure 1. The predicted secondary structure of the reported aptamer for chloramphenicol. Bases 46 to 50 were found to be consensus regions for binding to CAP.

3.2. Determination of secondary structures of curtailed oligonucleotides

For the aptamer to function as a specific receptor for binding, it has to fold into a secondary conformation which is a function of the nucleotide sequence. Reduction in length therefore changes the secondary structure and may affect molecular recognition. It was specifically necessary to predict if the hairpin bend in the binding consensus region would form [22].

The secondary structures and circular plots of the curtailed oligonucleotides were generated by Mfold (Figure 2). Wherever multiple structures were generated, the most stable configuration (as inferred from the ΔG) was selected. It can be seen that the target-binding hairpin loop is present in all the structures, supported by the circular plots (two distinct cytosine – guanine triple bonds). This proves that the structure plays a crucial role in stability and recognition [30]. However, the other regions and their interactions vary largely with longer truncations (sequences 5 to 11). Sequences 7 and 10 do not form any other secondary structure except the hairpin.

Preprints (www.preprints.org) | NOT PEER-REVIEWED | Posted: 29 April 2023 doi:10.20944/preprints202304.1208.v1

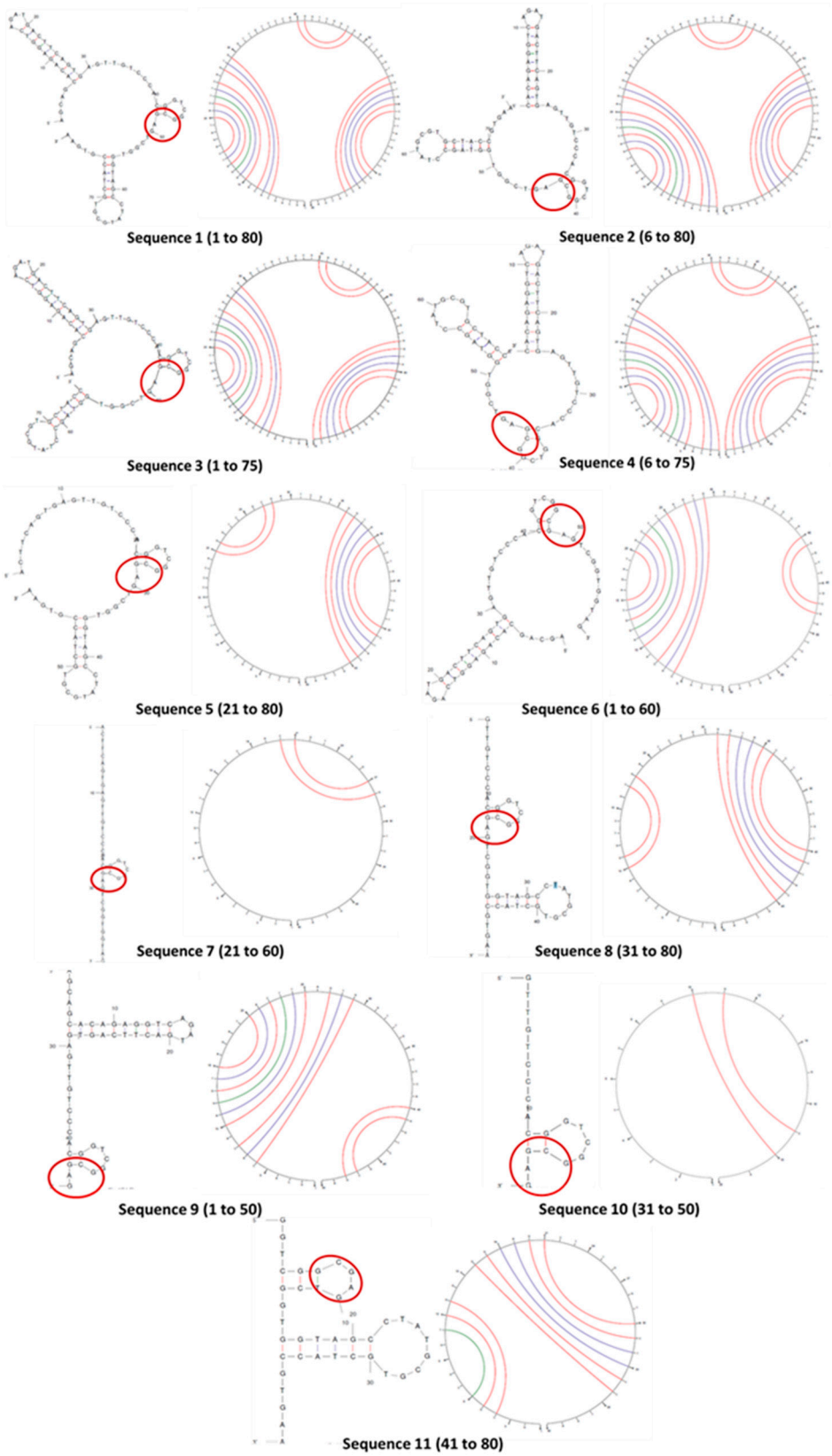

Figure 2. The folded secondary structures and circular plots of Sequences 1 to 11. The arcs in the circular plots join the bases that hybridize in the duplex structure. The consensus region in the secondary structures are circled in red.

Preprints (www.preprints.org) | NOT PEER-REVIEWED | Posted: 29 April 2023 doi:10.20944/preprints202304.1208.v1

3.3. Stability of curtailed oligonucleotides

Stable folding relies on the energetics, that is, ΔG and ΔS of the molecules, and Tm of the duplexes [24,25]. These parameters are dependent on nucleotide base stacking, electrostatic repulsion between negative bases, rigidity of conformation, hydrogen bonding between complementary bases and hydrogen bonding between nucleotides and solvent water [31].

Although structural stability does not directly affect aptamer affinity, this study corroborates our secondary structure predictions. We observed less change in thermodynamic properties where secondary structures were absent (Figure 3). Low ΔH de-stabilizes base stacking and pairing, whereas less (-)ΔS change depicts insignificant conformational change on solvation of oligonucleotides in water.

Sequences 1 to 4 differ by 5 or 10 bases from each other, with similar energetics and stable folding in solution (a high negative ΔG and a less negative ΔS). Pattern of and ability to form duplexes are similar too (Tm and structures in Figure 2). Since the goal of curtailing was to considerably shorten aptamers retaining conformational stability, sequences 5 to 11 were minutely studied. The duplexes were quite stable with Tm between 53.1 and 58.5 °C. Sequences 5, 6, 8 and 9 showed quite high (-)ΔG and ΔH, and comparatively lower (-)ΔS, signifying good base stacking and solvation. For sequences 7, 10 and 11, ΔG and ΔH values decrease sharply, suggesting poor conformational stability. Sequences 7, 11 have 40 bases, and 10 has only 20 bases, signifying that drastic truncation of aptamers strongly effect their folding.

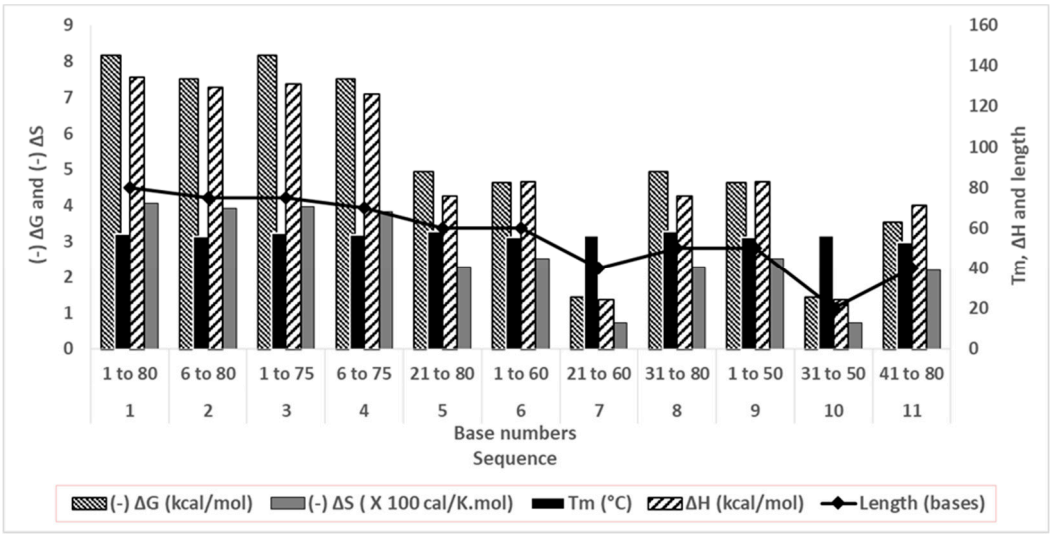

Figure 3. Thermodynamic parameters of folding of truncated oligonucleotides in correlation with their lengths.

3.4. Binding affinity with analyte

The crucial factor of aptamer-analyte binding affinity was studied next using BLI [32]. BLI offers advantage over surface plasmon resonance or optical waveguide based kinetic measurements, since it uses a static microfluidic system, without requirement of sample flow across a sensor. A wellplate is agitated to mimic fluidics (Figure S1) leading to simple, quick and high-throughput measurement of kinetics [32,33].

The aptamer is first loaded onto probes (Figure S2), then CAP is allowed to attach to aptamers (association) and then stripped off from it (dissociation) (refer Supplementary Information). Since the binding capacities of oligonucleotides differ, the association time was varied to allow complete capture (x-axis, Figure 4). For the same reason the magnitude of the shift has also varied (y-axis, Figure 4). The best fit among replicates were selected. The data was subjected to local curve fitting (shown in red) following 1:1 stoichiometric model. The choice of the final oligonucleotide was based on the regression coefficient of the fitting (R^2) and K_d (Table 2).

Preprints (www.preprints.org) | NOT PEER-REVIEWED | Posted: 29 April 2023 doi:10.20944/preprints202304.1208.v1

The original aptamer curve (Sequence 1) and sequences of similar length (2, 3 and 4) show high magnitude of shift and low noise. However, both the association and dissociation curves in these four cases have low slopes. These slopes are rate constants that are numerically denoted as k_{assoc} (association) and k_{dissoc} (dissociation). Low slopes denote that both binding and dissociation are gradual. The K_d values (which is a ratio of k_{dissoc} and k_{assoc}) for sequences 1 to 4, are higher due to low k_{assoc}.

A considerable difference in the curve patterns was observed for longer truncation. Removal of 20, 30 and 40 bases reduced the shift and introduced noise. The association and dissociation curves were steeper in some (sequences 6 and 8), but few were deviant from the model (low R^2). However, our goal was not only to lower K_d but also to reduce the aptamer length, so that aptamer doesn't bind strongly to both CAP and competing species. Therefore, the choice of aptamers was made from sequences 4 to 11. Sequence 9 was the best choice as the BLI curve showed lower noise, better R^2 and steeper association and flatter dissociation giving a K_d of 0.092 μM. However, Sequence 9 was still 50 bases long and it was important to check if similar and shorter oligonucleotides (7, 8, 10 and 11) displayed appreciable aptasensing efficiency. Sequence 10 bound weakly (low K_d and R^2) so it was eliminated from studies at this point. Sequences 7, 8, 9 and 11 were investigated for analytical performance.

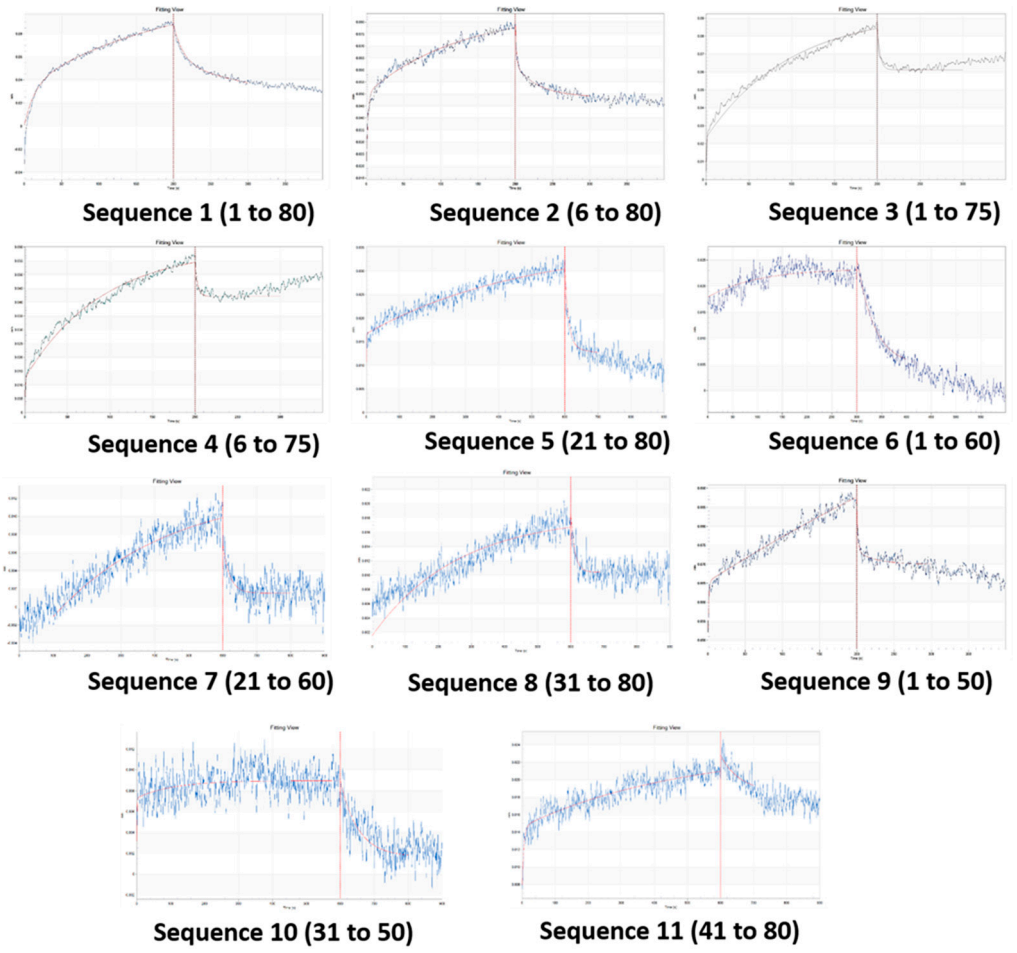

Figure 4. The fitted association-dissociation curves of the original and truncated oligonucleotides as obtained from biolayer interferometry assay (y-axis: spectral shift in nm, x-axis: time in sec).

Preprints (www.preprints.org) | NOT PEER-REVIEWED | Posted: 29 April 2023 doi:10.20944/preprints202304.1208.v1

Table 2. Characteristics of the aptamer-analyte binding and curve fitting using bio-layer interferometry.

Sl.no.	*Sequence number*	*K_d (μM)*	*R^2*
1	1	0.704 (previously reported value in literature is 0.766)	0.993
2	2	0.877	0.973
3	3	0.645	0.946
4	4	0.661	0.945
5	5	1.712	0.924
6	6	4.014	0.905
7	7	0.370	0.882
8	8	0.153	0.853
9	9	0.092	0.914
10	10	3.109	0.699
11	11	0.426	0.757

3.5. Aptasensing of CAP

3.5.1. Performance of the assay

With the original aptamer, resolution of the assay was unsatisfactory and 299.64 pg mL^{-1} of CAP in buffer could be accurately quantified [Figure S3]. With Sequence 9 and optimized concentrations, the response (A_{610}/A_{520}) was plotted against the logarithmic values of CAP concentrations. The linear range was found to be from 10 pg mL^{-1} to 10 μg mL^{-1}, with a resolution of 1 order of magnitude in concentration [Figure 5].

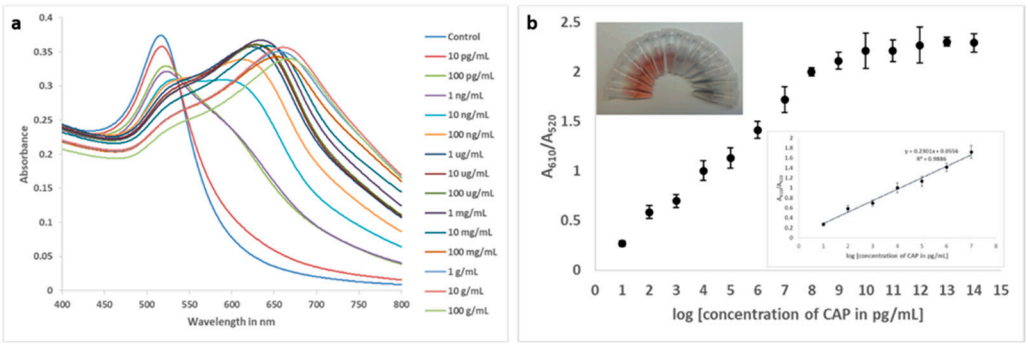

Figure 5. (a): Absorbance spectra of aptamer-gold nanoparticles with increasing concentrations of CAP. (b) The plot of the ratio of absorbance at 610 nm and 520 nm [Inset top: Photograph of colour change of gold nanocolloid with increasing concentration of CAP. Clockwise: Control, 1 pg mL^{-1} to 100 mg mL^{-1} with intervals of 1 order of magnitude. Inset bottom: The linear range of response] (n = 3).

The LOD and LOQ for the improved aptasensing were estimated to be 1.673 pg mL^{-1} (parts per trillion) and 5.563 pg mL^{-1}, respectively, in buffer with 9.8 % standard deviation of blank values for triplicate readings. The improvement in LOD achieved by aptamer truncation was calculated to be 179.10 times.

Performances of sequences 7, 8 and 11 were determined by quantifying recovery of different added concentrations of CAP in buffer (Table S1). Sequence 8 could sense CAP at lower concentrations (= 10 pg mL^{-1}), while the others could not accurately detect CAP at ultrasensitive levels (> 100 pg mL^{-1}). This clearly showed that the length (50 bases) and structure was important for binding and shorter sequences (40 and 20 bases) lacked good analytical potential. Such activity may be attributed to factors like conserved bases, types and number of secondary structures and length. The

Preprints (www.preprints.org) | NOT PEER-REVIEWED | Posted: 29 April 2023 doi:10.20944/preprints202304.1208.v1

original report on Sequence 1 mentioned that besides the consensus, there were two other discrete nucleotides that were conserved across the chosen aptamers [22]. These were guanine in 27th position and adenine in 39th position. Truncation resulted in the removal of guanine in Sequences 8 and 10 and both guanine and adenine in Sequence 11.

3.5.2. Validation in real samples

The colorimetric method was proven to be capable of ultrasensitive and accurate detection of CAP in real matrices. The accuracy was validated by standard HPLC method (Table 3). Recovery values ranged from 94.7 to 100.4%, with standard deviations in the range 3.8 to 8.6%.

Table 3. Recoveries of CAP from spiked honey samples determined by the truncated aptamer-mediated colorimetric method (n=3).

Sl.no.	Spiked amount (pg mL^{-1})	Aptasensing (pg mL^{-1})	HPLC (pg mL^{-1})	Recovery (%) ± SD (with respect to spiked amount)
1	0	Not detected	Not detected	-
2	10	9.66	Not detected	96.6 ± 2.7
3	100	94.77	Not detected	94.7 ± 3.8
4	1000	1004.28	Not detected	100.4 ± 6.9
5	10000	9812.50	9766.66	98.12 ± 1.1
6	50000	49605.71	48942.94	97.88 ± 8.6

3.5.3. Specificity and reproducibility

The relative standard deviation for the responses from the reproducibility investigation was found to be 2.44% for intra-day precision and 4.12% for inter-day precision, proving that the aptasensor was reproducible and stable.

Different analogues of CAP were subjected to the same bioanalysis and results showed high specificity for CAP (Figure 6), which may also be a result of stronger binding by the truncated aptamer.

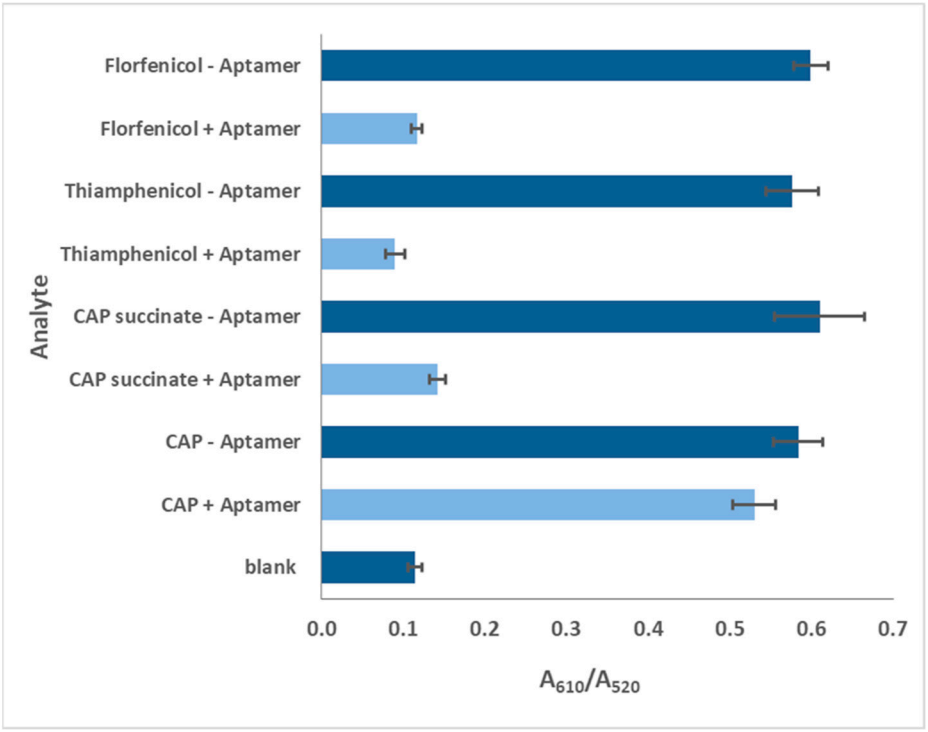

Figure 6. Responses of blank, 100 pg/mL of CAP, florfeniol, thiamphenicol and CAP succinate as recorded for the colorimetric assay.

Preprints (www.preprints.org) | NOT PEER-REVIEWED | Posted: 29 April 2023 doi:10.20944/preprints202304.1208.v1

3.5.4. Comparison with reported literature

A comprehensive compilation of reports published in the last five years on colorimetric aptasensing of CAP is presented in Table 4. Our aptasensing is among the most sensitive of them. Some authors [9,16] have reported lower LODs, probably achieved by target recycling and DNAzyme-hemin catalysis. One particularly notable method [13] employed ssDNA-based aptamer locking to counter the effect of length. The work by Tao et al 2020 [34] needs a special mention has they made a similar attempt to truncate the CAP aptamer to 40 nts. The shortened aptamer however was not desorbed from gold nanospheres in the presence of CAP, and therefore was not suitable for biosensing. The binding affinity could not be accurately measured by isothermal titration calorimetry. This study provides very useful insight into the choice of method to be used for K_d determination.

Several of these methods employ complicated, multi-step operations, two or more expensive biomolecules (complementary strands, chromogenic enzymes and substrates, antibodies, exonucleases, biotin-streptavidin, DNAzymes, single-stranded-binding proteins, hemin etc.) and multiple sets of nanoparticles for capture and signal amplification. Given the need for rapid, on-site detection of food and agricultural contaminants, few methods are particularly significant [10,11,13,14,17,18]. Our method is among them - one-step, simple, ultrasensitive with qualitative visual analysis and quantification by spectrophotometer or hand-held colorimeter.

Table 4. Previously reported colorimetric aptasensing of CAP.

Sl. no.	Detection principle	Significant features	Limit of detection (pg mL^{-1}) Real sample	Reference
1	Competitive Signalling molecule: TMB chromogen (enzymatic)	Capture probe attached to core-shell Fe@Au nanoparticles CAP competes with HRP labelled probe Requirement of functionalized core shell iron nanoparticles, gold nanoparticles, cDNA, HRP, substrates Multistep detection with magnetic separation	20 pg mL^{-1} (buffer) Fish Pork	9
2	Competitive Signalling molecule: TMB chromogen (enzymatic)	cDNA (complementary to aptamer) attached to Fe@Au nanoparticles. In presence of CAP, HRP labelled probe (with antibody) attaches to cDNA. Requirement of functionalized core-shell iron nanoparticles, cDNA, HRP, antibodies, substrates Multistep detection with magnetic separation	3 pg mL^{-1} (buffer) Fish Duck	10
3	Competitive Signalling molecule: TMB chromogen (enzymatic)	Aptamer attached to Fe@Au nanoparticles In presence of CAP, HRP labelled probe (with antibody) detaches from aptamer Requirement of functionalized core-shell iron nanoparticles, cDNA, HRP, antibodies, substrates Multistep detection with magnetic separation	15 pg mL^{-1} Fish	11
4	Competitive Signalling molecule: TMB chromogen (enzymatic)	Aptamer-cDNA-Pt-HRP conjugate attached to antibodies on Fe@Au nanoparticles In presence of CAP, cDNA-Pt-HRP HRP probe detaches from aptamer Exonuclease I used to cleave single strands releasing CAP (for recycling) and Pt-HRP (for signalling) Requirement of functionalized core-shell iron nanoparticles, Pt nanoparticles, cDNA, HRP and Exo I, antibodies, substrates Multistep detection with magnetic separation Recycling of target increases signal	0.30 pg mL^{-1} Milk	12

Preprints (www.preprints.org) | NOT PEER-REVIEWED | Posted: 29 April 2023 doi:10.20944/preprints202304.1208.v1

5	Competitive Signalling molecule: Gold nanoparticles	Free biotinylated aptamer binds to BSA on solid support, streptavidin-modified-DNA-nanoparticle conjugate attaches giving red colour. Colour fades when aptamer engaged by CAP Requirement of solid support, modification of aptamer (thiol, biotin), DNA to bind nanoparticles	145.67 pg mL^{-1} (buffer) 72.352 pg mL^{-1} (milk) 194.123 pg mL^{-1} (rat serum)	13
6	Protection of nanoparticles by aptamers Signalling molecule: Gold nanoparticles	Aptamers protected triangular nanoparticles are not etched to spherical particles Cu2+-assisted I−mediated method Simple one-step method with minimum components	1.62 x 10^6 pg mL^{-1} (buffer)	14
7	Competitive Signalling molecule: TMB chromogen (enzymatic)	Single stranded binding protein attached to Fe@Au nanoparticles Aptamer attached to SiO2@Au-HRP probe In presence of CAP, probe detached from magnetic nanoparticle complex Requirement of functionalized core-shell iron nanoparticles, functionalized core shell silica nanoparticles, SSB protein, HRP, substrates Multistep detection with magnetic separation	20 pg mL^{-1} Milk	15
8	Protection of nanoparticles by ssDNA Signalling molecule: Gold nanoparticles	Aptamer locked by short ssDNA in absence of CAP, leaving gold nanoparticles free for salt-induced aggregation Simple, one-step method, providing solution for long length of CAP aptamer	9.69 pg mL^{-1} (buffer) Milk	16
9	Competitive between CAP-base and CAP Signalling molecule: Gold nanoparticles	Negatively charged aptamer-functionalized gold nanoparticles aggregate in presence of positive CAP-base Presence of CAP leads to de-aggregation Simple, one-step detection	7.11 x 10^3 pg mL^{-1} (buffer) Spiked environmental water	17
10	Competitive Signalling molecule: TMB chromogen (enzymatic)	cDNA capture probe bound to microplate Aptamer tagged with HRP Requirement of binding to solid support by streptavidin, HRP, substrate	3.10 pg mL^{-1} Honey Fish	18
11	Competitive Signalling molecule: TMB chromogen (enzymatic)	Magnetic bead functionalized with aptamer cDNA-gold nanoparticle-hemin/G-quadruplex DNAzyme catalysed TMB conversion Requirement of complex functionalization of gold nanoparticles, cDNA, hemin, DNAzyme, substrates Multistep detection with magnetic separation	0.13 pg mL^{-1} (buffer) Milk	19
12	Competitive Signalling molecule: TMB chromogen (enzymatic)	Fe-based metal organic framework catalyses TMB conversion. Catalysis reduced if gold nanoparticle-aptamer-CAP complex binds to it Simple, easy transduction	8.1 x 10^3 pg mL^{-1} (buffer) Spiked tap water	20
13	Protection of nanoparticles by ssDNA Signalling molecule: Gold nanoparticles	Lanthanide attaches to aptamer functionalized gold nanoparticles and assists aggregation In presence of CAP, aptamer detaches from nanoparticles Simple, one-step detection Can be detected through instrument and smartphone imaging app	2.471 x 10^3 pg mL^{-1} (spectro-photometer) 1.899 x 10^3 pg mL^{-1} (smartphone app) Solid milk	21

			Chicken	
14	Protection of nanoparticles by aptamers Signalling molecule: Gold nanoparticles	Truncated aptamers bind to gold nanospheres in absence of CAP Unbound nanospheres aggregate in presence of salt, changing colour of colloid	1.67 pg mL^{-1} (buffer) Honey	***Present work***

4. Conclusions

A strong binding affinity between aptamer and analyte is imperative for biomonitoring. Lack of sensitivity in nanosphere-aggregation based colorimetric aptasensing of CAP prompted the present investigation of truncating the aptamer to improve its binding affinity – a first report for CAP aptamer. In silico evaluation and bio-layer interferometry showed that a 50-base oligonucleotide had stable configuration with stronger binding. This aptamer improved detection limit by 32.87 times. Earlier literature on CAP aptasensing employs multiple recognition, amplification and capture molecules, several steps and complicated assay format. Our work is the first on non-cross-linked aggregation of nanospheres for CAP detection. It boasts of simple, visual yet ultrasensitive detection. Given the serious threats posed by antibiotics in food and the necessity of field-applicable convenient analysis, ours is a promising biosensing technique. It will enable identification of minute traces of the antibiotic possibly facilitating prevention of its entry into the food chain and subsequent health hazards.

Supplementary Materials: The following supporting information can be downloaded at the website of this paper posted on Preprints.org.

Author Contributions: Conceptualization, R.S and P.B..; methodology, R.S, M.M. and P.B.; validation, R.S, P.B. and K.R.; formal analysis, R.S.; investigation, R.S., M.M. and P.B..; resources, P.B. and K.R.; data curation, R.S.; writing—original draft preparation, R.S.; writing—review and editing, R.S., M.M., P.B. and K.R.; supervision, P.B. and K.R.; funding acquisition, P.B. All authors have read and agreed to the published version of the manuscript.

Funding: This research received no external funding.

Institutional Review Board Statement: Not applicable.

Informed Consent Statement: Not applicable.

Data Availability Statement: Data will be available on request.

Acknowledgments: The authors thank Director, CSIR-CFTRI for the facilities provided for this work. RS and MM thank Council for Scientific and Industrial Research (CSIR) and Department of Science and Technology (DST-INSPIRE) for research fellowships. We gratefully acknowledge guidance in BLI experiments provided by Mr. Susheelendra Vaidya, Pall India Pvt. Ltd.; support from Department of Biotechnology, India for funding the BLI instrument and CeNSE, IISc facilities funded by MHRD and DST Nano Mission for TEM studies.

Conflicts of Interest: The authors declare no conflict of interest.

References

[1] Li J., Shao B., Shen T., Wang S. and Wu Y. Occurrence of Chloramphenicol-Resistance Genes as Environmental Pollutants from Swine Feedlots. Environ. Sci. Technol. 2013, 47 (6), 2892–2897

[2] Extralabel Drug Use in Animals, Fed. Regist. 1994, 61,57732–57745

[3] Durham M. A bitter taste of honey. The Guardian (International Edition). 21 Jul 2004. Accessed on 16th July 2018.

[4] Moudgil P., Bedi J. S., Aulakh R. S., Gill J. P. S., Kumar A. Validation of HPLC multi-residue method for determination of fluoroquinolones, tetracycline, sulphonamides and chloramphenicol residues in bovine milk. Food Anal. Methods. 2019, 12, 338–346

[5] Sharma R., Raghavarao KSMS. Nanoparticle-based aptasensors for food contaminant detection, in: Nanomaterials for Food Applications, A.L. Rubio et al. (eds.), Elsevier Inc. 2019, 123-145

[6] Gao H., Gan N., Pan D., Chen Y., Li T., Cao Y., Fu T. A sensitive colorimetric aptasensor for chloramphenicol detection in fish and pork based on the amplification of a nano-peroxidase polymer, Anal. Methods. 2015a, 7, 6528-6536

[7] Gao H., Pan D., Gan N., Cao J., Sun Y., Wu Z., Zeng X. An aptamer-based colorimetric assay for chloramphenicol using a polymeric HRP-antibody conjugate for signal amplification. Microchim. Acta. (2015a) 182, 2551–2559

[8] Miao Y., Gan N., Li T., Zhang H., Cao Y., Jiang Q. A colorimetric aptasensor for chloramphenicol in fish based on double-stranded DNA antibody labeled enzyme-linked polymer nanotracers for signal amplification. Sens. Actuators B Chem. (2015a) 220, 679–687

[9] Miao Y., Gan N., Ren H-X., Cao Y., Hu F., Yan Z., Chen Y. A triple-amplification colorimetric assay for antibiotics based on magnetic aptamer–enzyme co-immobilized platinum nanoprobes and exonuclease-assisted target recycling. Analyst. 2015b 140, 7663-7671

[10] Abnous K., Danesh N. M., Ramezani M., Emrani A. S., Taghdisi S. M. A novel colorimetric sandwich aptasensor based on an indirect competitive enzyme-free method for ultrasensitive detection of chloramphenicol. Biosens. Bioelectron. 2016, 78, 80–86

[11] Chang CC., Wang G., Takarada T., Maeda M. Iodine-mediated etching of triangular gold nanoplates for colorimetric sensing of copper ion and aptasensing of chloramphenicol. ACS Appl. Mater. Interfaces. 2017, 9, 34518−34525

[12] Luan Q., Xi Y., Gan N., Cao Y., Li T., Chen Y. A facile colorimetric aptamer assay for small molecule detection infood based on a magnetic single-stranded DNA binding protein-linked composite probe. Sens. Actuators B Chem. 2017, 239, 979–987.

[13] Javidi M., Housaindokht M. R., Verdian A., Razavizadeh B. M. Detection of chloramphenicol using a novel apta-sensing platform based on aptamer terminal-lock in milk samples. Anal. Chim. Acta 2018, 1039, 116-123

[14] Xie Y., Huang Y., Tang D., Cui H., Cao H.A. competitive colorimetric chloramphenicol assay based on the non-cross-linking deaggregation of gold nanoparticles coated with a polyadenine-modified aptamer, Mikrochim Acta, 185 (12), 534

[15] Yan C., Zhang J., Xue F., Lu J., Li B., Chen W. Aptamer-mediated colorimetric method for rapid and sensitive detection of chloramphenicol in food. Food Chem. 2018, 260, 208–212

[16] Huang W., Zhang H., Lai G., Liu S., Li B., Yu A. Sensitive and rapid aptasensing of chloramphenicol by colorimetric signal transduction with a DNAzyme-functionalized gold nanoprobe. Food Chem. 2019, 270, 287-292

[17] Li J., Yu C., Wu Y-n., Zhu Y., Xu J., Wang Y., Wang H., Guo M., Li F. Novel sensing platform based on gold nanoparticle-aptamer and Fe-metalorganic framework for multiple antibiotic detection and signal amplification. Environ. Int. 2019, 125, 135–141.

[18] Wu Y-y., Liu, B-w., Huang, P., Wu, F-y. A novel colorimetric aptasensor for detection of chloramphenicol based on lanthanum ion–assisted gold nanoparticle aggregation and smartphone imaging. Anal Bioanal Chem. 2019, 411(28), 7511-7518

[19] Sharma R., Ragavan K.V., Raghavarao K.S.M.S., Thakur M.S. Nano-aptamer based quantitative detection of chloramphenicol in: Biotechnology and Biochemical Engineering, Select Proceedings of ICACE 2015, B.D. Prasanna et al. (eds.), Springer, 2016, 187-195

[20] McKeague M., DeRosa M. C. Challenges and opportunities for small molecule aptamer development. J. Nucleic Acids, 2012. 748913, 20 pages.

[21] Duan, Y., Gao, Z., Wang, L., Wang, H., Zhang, H., and Li, H. Selection and identification of chloramphenicol-specific DNA aptamers by Mag-SELEX. Appl. Biochem. Biotechnol. 2016, 180(8), 1644-1656.

[22] Mehta, J., Van Dorst, B., Rouah-Martin, E., Herrebout, W., Scippo, M. L., Blust, R., Robbens, J. In vitro selection and characterization of DNA aptamers recognizing chloramphenicol. J. Biotechnol. 2011, 155(4), 361-369.

[23] Zuker, M. Mfold web server for nucleic acid folding and hybridization prediction. Nucleic Acids Res. 2003, 31(13), 3406-3415.

[24] Searle, M. S., Williams, D. H.. On the stability of nucleic acid structures in solution: enthalpy-entropy compensations, internal rotations and reversibility. Nucleic Acids Res. 1993, 21(9), 2051-2056.

[25] Owczarzy, R., You, Y., Groth, C. L., and Tataurov, A. V. Stability and mismatch discrimination of locked nucleic acid–DNA duplexes. Biochemistry, 2011, 50(43), 9352-9367.

[26] Yang Y., Yin Y., Li X., Wang S., Dong Y. Development of a chimeric aptamer and an AuNPs aptasensor for highly sensitive and specific identification of Aflatoxin B1,Sens. Actuators B Chem. 2020, 319, 128250

[27] Alawad A., Istamboulié G., Calas-Blanchard C., Noguer T. A reagentless aptasensor based on intrinsic aptamer redox activity for the detection of tetracycline in water, Sens. Actuators B Chem. 2019, 288, 141-146

[28] Macdonald, J. Houghton, P. Xiang, D. Duan, W., Shigdar, S. Truncation and mutation of a transferrin receptor aptamer enhances binding affinity. Nucleic Acid Therapeutics. 2016, 26, 6, 348-354

[29] Sun, Y., Duan, N., Ma, P., Liang, Y., Zhu, X., Wang, Z. Colorimetric aptasensor based on truncated aptamer and trivalent DNAzyme for Vibrio parahemolyticus determination, J. Agric. Food Chem. 2019. 67, 8, 2313–2320

[30] Sharma, R., Akshath, U.A.S., Bhatt, P., Raghavarao, KSMS. Fluorescent aptaswitch for chloramphenicol detection -quantification enabled by immobilization of aptamer, Sens. Actuators B Chem. 2019, 290, 110-117

[31] Abnous K., Danesh N.M., Ramezani M., Taghdisi S.M., Emrani A.S. A novel electrochemical aptasensor based on H-shape structure of aptamer-complimentary strands conjugate for ultrasensitive detection of cocaine, Sens. Actuators B Chem. 2016, 224, 351-355

[32] Auer S., Koho T., Uusi-Kerttula H., Vesikari T., Blazevic V., Hytönen V.P. Rapid and sensitive detection of norovirus antibodies in human serum with a biolayer interferometry biosensor, Sens. Actuators B Chem. 2015, 221, 507-514

[33] Gandhi, I., Narendran, K., Jackson, G.W. Rapid DNA Aptamer Binding Characterization and ELASA Development Using Biolayer Interferometry (BLI). https://www.basepairbio.com. 2011, Accessed on: 17th January 2017.

[34] Tao, X., He, F., Liu, X., Zhang, F., Wang, X, Peng, Y., Liu, J. Detection of chloramphenicol with an aptamer-based colorimetric assay: critical evaluation of specific and unspecific binding of analyte molecules. Microchim Acta 2020, 187, 668.